Aerosol and Air Quality Research, 15: 1506–1513, 2015

ISSN: 1680-8584 print / 2071-1409 online
doi: 10.4209/aaqr.2014.12.0334

Improving the Removal Efficiency of Elemental Mercury by Pre-Existing Aerosol Particles in Double Dielectric Barrier Discharge Treatments

Qing Li[1], Jingkun Jiang[1,2*], Lei Duan[1], Jianguo Deng[1], Lun Jiang[3], Zhen Li[1], Jiming Hao[1,2]

[1] *State Key Joint Laboratory of Environment Simulation and Pollution Control, School of Environment, Tsinghua University, Beijing, 100084, China*
[2] *State Environmental Protection Key Laboratory of Sources and Control of Air Pollution Complex, Beijing 100084, China*
[3] *Department of Engineering Physics, Tsinghua University, Beijing 100084, China*

ABSTRACT

Plasma technology has been employed for the removal of gaseous elemental mercury (Hg^0) from simulated flue gases without pre-existing airborne particles. This study developed a double dielectric barrier discharge (DDBD) treatment system, in which two coaxial electrodes were covered by quartz dielectrics, for removing mercury with the presence of aerosol particles. The increase in pre-existing aerosol surface concentration can improve Hg^0 removal efficiency up to 160% in the DDBD device. Inorganic aerosol particles (sodium chloride) perform better than organic ones (sucrose) in improving Hg^0 removal efficiency. These aerosol particles can be collected in the DDBD system. For sodium chloride particles, a collection efficiency of more than 90% was observed in the tested diameter range of 10–100 nm. The improvement in Hg^0 removal with the presence of particles is possibly due to that (i) aerosol particles provide additional surface for surface-induced Hg^0 oxidations, (ii) reactive species (such as Cl) generated by plasma etching particle surface rapidly react with Hg^0, and (iii) charged particles can in-flight adsorb mercury species.

Keywords: Mercury removal; Aerosol particles; Plasma; DDBD; Pollution control.

INTRODUCTION

Mercury pollution has attracted growing concern owning to its negative effects on the environment and human health (Parks *et al.*, 2013). Many technologies have been developed for mercury control (Biswas *et al.*, 1999), such as injecting powdered activated carbon to adsorb mercury (Sjostrom *et al.*, 2010; Clack, 2012), injecting halogen reagents (Zhao *et al.*, 2006) and using UV light and ozone to realize mercury oxidization (Wu *et al.*, 1998; Granite and Pennline 2002; Lee *et al.*, 2004; McLarnon *et al.*, 2005; Wang *et al.*, 2007; Yang *et al.*, 2012). Non-thermal plasma operated at atmospheric pressure is one of the promising technologies for converting gaseous elemental mercury (Hg^0) to oxidized mercury (Hg^{2+}) and particulate bound mercury (Hg_p) (Chen *et al.*, 2006; Byun *et al.*, 2011a), which can then be effectively removed by conventional air-pollution control devices (Clack, 2006). Most of the electrical energy of non-thermal plasmas is consumed to produce UV and reactive species such as O_3, H_2O_2, radicals of OH, HO_2, and O (Jia *et al*., 2013; Li *et al.*, 2012). These reactive species and UV can oxidize Hg^0 at a high reaction rate. These species have also been recognized for potentially oxidizing NO and SO_2 from flue gas (Liang *et al.*, 2002; Jeong and Jurng 2007; Xu *et al.*, 2009), destructing carbonyl sulfide (Tsai *et al.*, 2007), and removing organic compounds (Chang and Hsieh 2013; Lin *et al.*, 2013).

The application of non-thermal plasma technology for mercury removal has been mainly studied with corona discharge (Ko *et al.*, 2008; Byun *et al.*, 2011b) and dielectric barrier discharge system (Chen *et al.*, 2006; Jeong and Jurng, 2007; Byun *et al.*, 2011a). Both kinds of plasma treatment systems employed one naked metal electrode (commonly as the high voltage electrode), which can partially heat the flue gas, resulting in the unnecessary consumption of electrical energy. In a recent study, surface discharge plasma injection approach (naked electrode for discharge in the reactor) was proposed for oxidizing Hg^0 (An *et al.*, 2014). Its challenge is that the naked metal electrode will be etched over a long-term continuous operation. In addition, to the best of our knowledge, previous investigations on non-thermal plasma treatment of simulated flue gases did not include aerosol particles, which always co-exist with mercury in real flue gases.

The objective of this study was to develop a non-thermal plasma device with double dielectric barrier discharge (DDBD) configuration, in which two coaxial electrodes

* Corresponding author.
E-mail address: jiangjk@tsinghua.edu.cn

were covered by quartz dielectrics, for a low-consumption of electrical energy and no-consumption of metal electrodes. Aerosol particles were included in the simulated flue gases to examine their role in mercury removal. Both inorganic (sodium chloride) and organic (sucrose) particles were tested. Possible mechanisms for the role of aerosol particles in mercury removal were discussed. Furthermore, the collection efficiency of these aerosol particles by the plasma device was investigated.

EXPERIMENTAL DESCRIPTION

Fig. 1 shows a schematic diagram of the experimental setup and a typical discharge photo. The DDBD device is made by two quartz cylinders with the height between the inlet and the upper lid of ~18 cm, while the gap (discharge region) between the two cylinders is 2.0 mm. A copper band with the width 2.0 cm surrounds the outside surface of the outer cylinder in four loops as the ground electrode, which is covered with silicon vacuum grease to avoid discharge in the outside surface. Another copper band fully covers the inside surface of the inner cylinder as the power electrode, which is connected to a high voltage power supply (CW1003, Nantong Sanxin, China) with a fixed voltage frequency of 10.0 ± 0.6 kHz. Its output power, monitored by a power meter, can be controlled by adjusting the output voltage amplitude in the range of 0.5–20 kV. The input energy density was obtained by dividing the output power with the volume of the discharge region. A stainless steel heat sink is placed in the middle of the inner cylinder for cooling the power electrode. The gap between the heat sink and the power electrode is filled with silicone oil to avoid discharge inside the inner cylinder. The inlet for incoming flue gas is at the outside bottom while the outlet for outgoing flue gas is at the outside top. A hopper is jointed in the bottom to collect dust and cooling water from the flue gas. This design of DDBD configuration, only discharging between two quartz dielectric surfaces, ensures a long-term continuous operation with no-consumption of metal electrodes.

The flow rates of incoming simulated flue gases were controlled by mass flow meters. Aerosol particles were generated by an atomizer. Both inorganic (sodium chloride) and organic (sucrose) particles were produced. Aerosol surface area concentration was adjusted by using solutions with different concentrations. Hg^0 was introduced by passing nitrogen through a mercury permeation tube. Its concentration was controlled by the water bath temperature (15–38°C). Humidity and temperature of the incoming gases were adjusted by a moistener and a heating tape, respectively. The tubing temperature was fixed at 65°C by controlling the power supplied to the heating tape surrounding the tubing. All the incoming gases were mixed before entering the DDBD device. The residence time of the simulated flue gases in the DDBD chamber was ~0.25 s. After the DDBD treatment, Hg^0 concentration (C_{Hg0}) was monitored by an Hg^0 analyzer (Lumex RA-915+, Ohio Lumex Company, Inc., St. Petersburg, Russia). Its lower detection limit is ~0.1 $\mu g/m^3$. An ice bath was used to cool down the flue gas after the plasma device. A membrane filter was used to remove particles prior to Hg^0 measurement. Since residue ozone generated by plasma can absorb ultraviolet with the wavelength of 254 nm and affect Hg^0 measurement. Melanterite ($FeSO_4 \cdot 7H_2O$) powders, converting ozone to oxygen (Logager *et al.*, 1992), were used for adsorbing residual ozone (O_3) prior to Hg^0 measurement. Elementary mercury concentration was monitored at the outlet of the DDBD device with it being on and off. Hg^0 removal efficiency was then defined as 1 – (C_{Hg0} when DDBD turns on)/(C_{Hg0} when DDBD turns off).

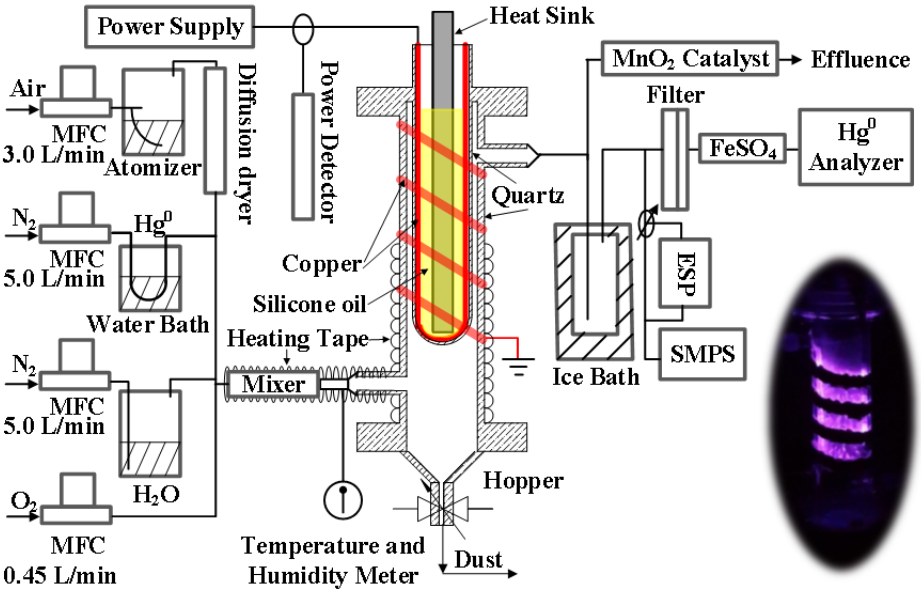

Fig. 1. Schematic of experimental setup and a typical plasma discharge photo (in the lower right corner). The red color lines denote electrodes made of copper, while the yellow color band denotes silicon oil in the inner quartz tube. MFC: mass flow controller; ESP: electrostatic precipitator; SMPS: scanning mobility particle sizer.

A scanning mobility particle sizer (SMPS 3936, TSI Inc., USA) was used to measure aerosol size distributions at the outlet of the DDBD device. Tygon tubing was used between the reactor outlet and the SMPS inlet to minimize aerosol losses (Liu *et al.*, 1985). Fig. 2 shows typical size distributions of sodium chloride aerosol generated in this study. Sucrose aerosol had similar size distributions. Total aerosol surface concentrations were estimated by assuming that particles are spherical. Total surface concentrations of 0.1×10^{11}, 0.4×10^{11}, and 1.2×10^{11} nm^2/cm^3 were tested in this study, while their corresponding peak diameters were about 40, 49, and 67 nm, respectively. A homemade electrostatic precipitator (ESP; a coaxial cylinder with the inner electrode diameter of 0.45 cm, the gap of 0.1 cm, and the length of 40 cm; its collection efficiency for sub-200 nm charged particles was higher than 95% when a high voltage of 1 kV was supplied) was set as a bypass before SMPS. The collection efficiency at a given particle diameter is defined as 1 – ($C_{particle}$ when DDBD turns on)/($C_{particle}$ when DDBD turns off) with ESP turns off, while the enhanced collection efficiency by the ESP at a given particle diameter is defined as 1 – ($C_{particle}$ when DDBD turns on)/($C_{particle}$ when DDBD turns off) with ESP turns on. Particle concentration, $C_{particle}$, was derived from aerosol size distribution measured by the SMPS.

RESULTS AND DISCUSSIONS

Improving Mercury Removal Efficiency by Adding Aerosol Particles

Fig. 3(a) shows Hg^0 removal efficiency as a function of input energy density in the DDBD device with different NaCl aerosol surface concentrations. An increase in input energy density results in a higher Hg^0 removal efficiency. However, the removal efficiency appears to reach a plateau at a certain input energy density, e.g., ~15, 11, 9.5, 8.5 J/L for NaCl aerosol surface concentration of 0, 0.1×10^{11}, 0.4×10^{11}, and 1.2×10^{11} nm^2/cm^3, respectively. A continuous increase in input energy increases electrical energy cost. These findings are consistent with results reported in plasma systems using corona discharge and single dielectric barrier discharge (Chen *et al.*, 2006; Jeong and Jurng, 2007; Ko *et al.*, 2008; Wang *et al.*, 2010). Furthermore, these findings show that pre-existing NaCl particles improve Hg^0 removal efficiency. The efficiency enhancement is ~160% at the input energy density of ~9 J/L. An increase in aerosol surface concentration leads to a higher Hg^0 removal efficiency.

Fig. 3(b) shows Hg^0 removal efficiency as a function of input energy density in the DDBD device with the existence of sucrose particles. The tendency with increasing input energy density is similar. However, the enhancement in Hg^0 removal by sucrose particles doesn't increase monotonically with increasing aerosol surface concentration. Hg^0 removal efficiencies at sucrose aerosol surface concentration of 1.2×10^{11} nm^2/cm^3 are lower than those at a lower aerosol surface concentration of 0.4×10^{11} nm^2/cm^3.

Results shown in Fig. 3 were obtained at the incoming Hg^0 concentration of 110 $\mu g/m^3$. Fig. 4 compares the effect of sodium chloride and sucrose particles at other Hg^0 concentrations, i.e., 45 and 210 $\mu g/m^3$. Consistent results were observed. Pre-existing NaCl particles perform better in improving Hg^0 removal efficiency than sucrose particles,

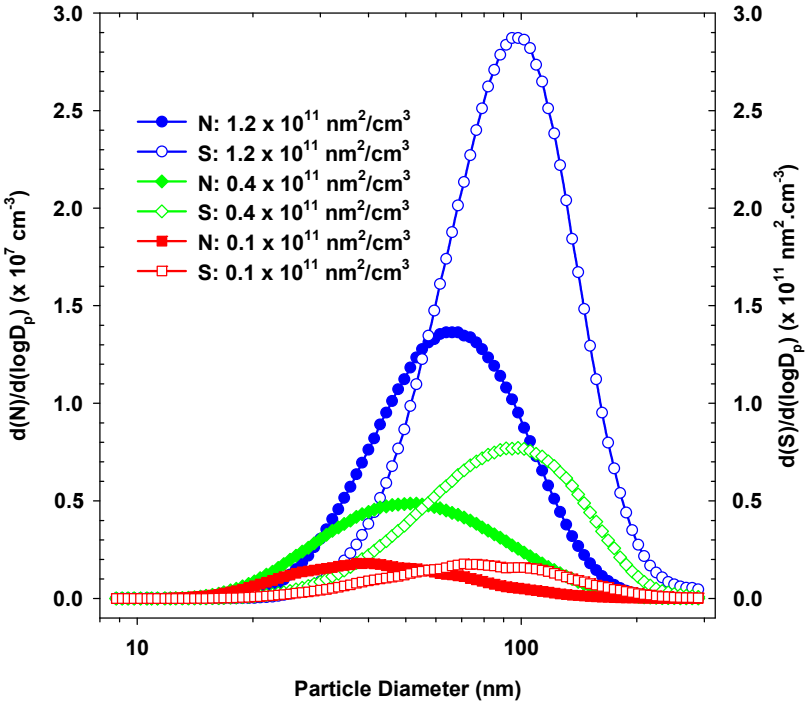

Fig. 2. Typical distributions of sodium chloride particle number (N) and surface (S) concentrations with the function of particle diameter for three aerosol surface concentrations: 0.1×10^{11}, 0.4×10^{11}, and 1.2×10^{11} nm^2/cm^3, respectively.

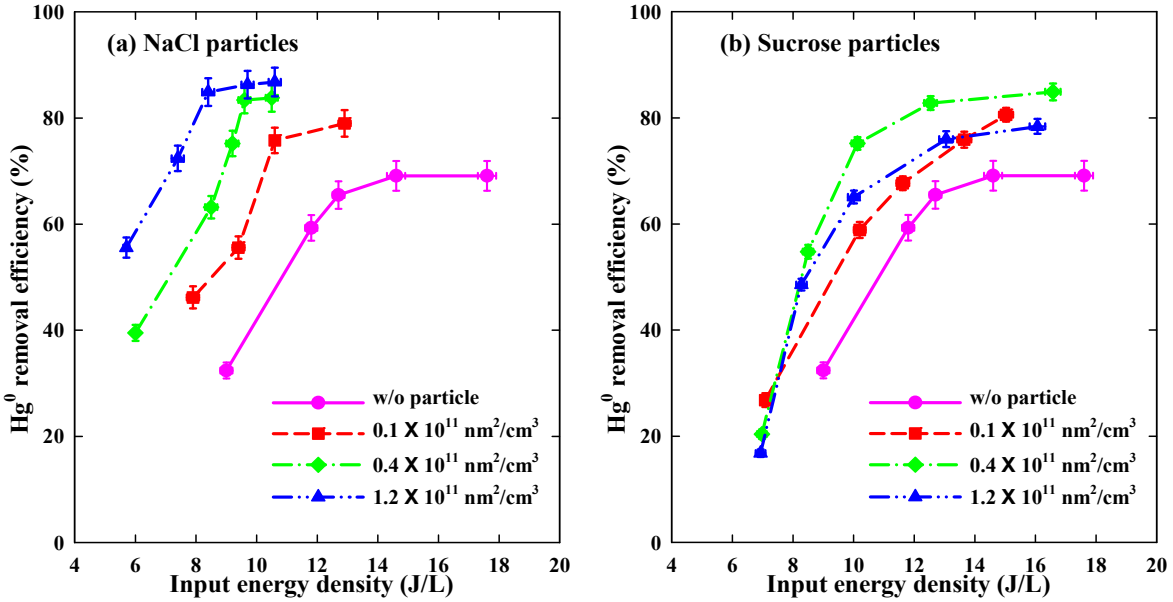

Fig. 3. Hg^0 removal efficiency as a function of input energy density in the plasma process with different (a) NaCl and (b) sucrose aerosol surface concentrations. For comparison, the solid pink line shows the result without pre-existing aerosol particles. Gas conditions: 8% O_2 and 4% H_2O in N_2 balance; incoming Hg^0 concentration fixed at 110 μg/m^3.

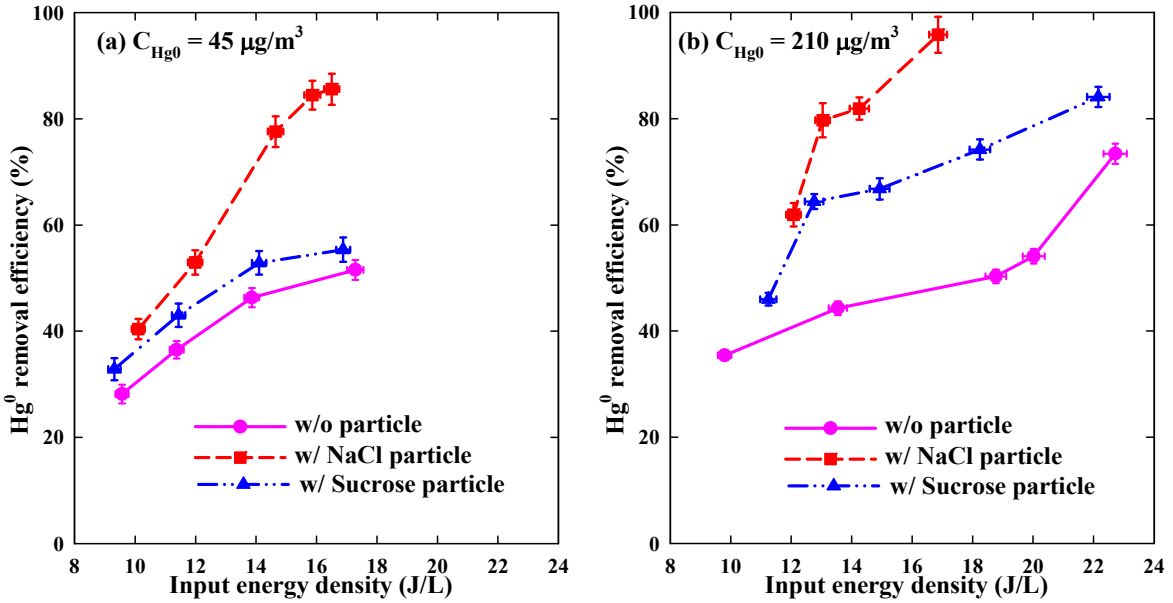

Fig. 4. The effect of aerosol type on mercury capture in the plasma system. The incoming Hg^0 concentration was (a) 45 μg/m^3 (b) 210 μg/m^3 with aerosol surface concentration of 0.4 × 10^{11} nm^2/cm^3. The solid pink line shows the result without pre-existing aerosol. Gas conditions: 8% O_2 and 4% H_2O in N_2 balance.

especially at high input energy density (such as > 14 J/L). Another inorganic particles, $(NH_4)_2SO_4$, were also tested in this study and showed similar characteristics as NaCl particles with a slightly lower Hg^0 removal efficiencies.

Collection Efficiency of Aerosol Particles

Fig. 5(a) shows collection efficiencies of sodium chloride particles by the DDBD device with and without the downstream ESP. A higher energy input in the DDBD device results in a higher particle collection efficiency. When the downstream ESP was used, most charged aerosol particles from the reactor outlet were captured. When particle diameter is smaller than ~15 nm, the collection efficiency drops significantly because of their low charging efficiency (Jung and Kittelson, 2005; Jiang *et al.*, 2007a, b; Suriyawong *et al.*, 2008) and possibly related to the generation of new particles in the plasma region as well (Romay *et al.*, 1994; Guo *et al.*, 2014). Most pre-existing NaCl particles (> 90% in particle number) were collected. The charged ratio of aerosol particles in the outgoing gases was over 50% in the

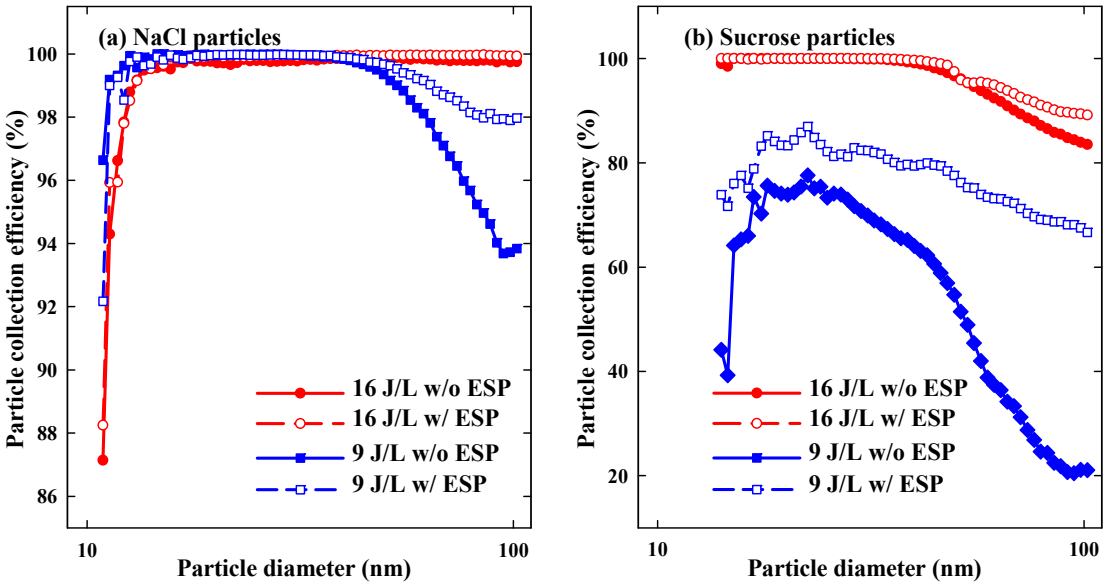

Fig. 5. Particle collection efficiency by the double dielectric barrier discharge device with and without a downstream electrostatic precipitator. The incoming Hg^0 concentration was 110 μg/m^3. Pre-existing (a) NaCl and (b) sucrose aerosol surface concentration was 0.4×0^{11} nm^2/cm^3.

particle diameter range of 30–100 nm, according to results with and without the ESP.

Fig. 5(b) shows collection efficiencies of sucrose particles by the DDBD device. The result for sub-15 nm particles is not shown due to bad repetition in experiment. The tendency of the collection efficiency as a function of particle diameter is similar to that of NaCl particles. However, the collection efficiencies are much lower than those of NaCl particles, especially at low input energy density, e.g., 9 J/L.

Possible Mechanisms for Improving Mercury Removal in the DDBD System

Schematic illustration for possible Hg^0 removal mechanism in the DDBD system with pre-existing aerosol particles is shown in Fig. 6, i.e., Hg^0 oxidized by plasma species directly in gas-phase and on aerosol surface, and Hg^0 in-flight adsorbed by charged aerosol particles.

Firstly, Hg^0 can be directly oxidized by plasma species (e.g., •OH and O radicals) in discharge and post-discharge regions to form oxidized mercury (Hg^{2+}). This process is the major removal pathway of Hg^0 when there are no suspended particles in the flue gas. When aerosol particles are present, the etching of particle surface by plasma may generate reactive species as well. For instance, Cl might be produced when NaCl particles are present. As one of the most common composition in flue gas from coal combustion (Saarnio *et al.*, 2014), Cl has been reported for rapidly reacting with Hg^0 in gas phase and on the particle surface to form oxidized mercury (Zhao *et al.*, 2006; An *et al.*, 2014). Possibly due to this mechanism, NaCl aerosol performs better in improving Hg^0 removal than sucrose aerosol.

Secondly, pre-existing aerosol particles provide additional surfaces for Hg^0 oxidation reactions. Experimental investigation without pre-existing aerosol particles found that most of the removed Hg^0 deposits on plasma reactor surface in the form of oxidized mercury (Byun *et al.*, 2011a; An *et al.*, 2014;). Surface-induced reaction has higher reaction rate than that of gas-phase oxidation reaction (Pal and Ariya, 2004). The effect of surface-induced reaction can be enhanced due to the addition of surface area by suspended aerosol particles in the plasma region.

Thirdly, suspended particles possibly in-flight adsorb mercury, especially for charged particles and mercury ions. The plasma process can lead to aerosol charging (Manirakiza *et al.*, 2013), while Hg^0 can be ionized to mercury ions (Hg^+, Hg^{2+}) due to the lower first ionization energy of elemental mercury (10.4 eV) than that of most common flue gas molecules such as N_2 and O_2. The charged aerosol particles can then in-flight adsorb mercury (Clack, 2006), especially for mercury ions. Our experimental results reveal that NaCl particles of higher charged fractions have better mercury removal efficiencies than sucrose particles of relatively lower charged fractions.

Pre-existing aerosol particles provide reaction surface for heterogeneous nucleation and increase condensation of condensable species (McMurry *et al.*, 2005; Kuang *et al.*, 2010). Formed Hg_p can be collected by the DDBD device and/or removed by the downstream conventional air pollution control system such as ESP. This enhanced removal of mercury is possibly magnified in stage ESP systems which include a dielectric barrier discharge configuration for pre-charging aerosol particles (Byeon *et al.*, 2006).

Except for the above processes, the reaction of plasma species with aerosol particles cannot be ignored, especially for organic particles whose surface oxidation can compete for the reactive species. The highly reactive species can oxidize and etch aerosol surface, resulting in aerosol evaporation and shrink to form new molecules and smaller aerosol particles. The newly formed molecules and/or particles can also compete for plasma-generated reactive species. It is

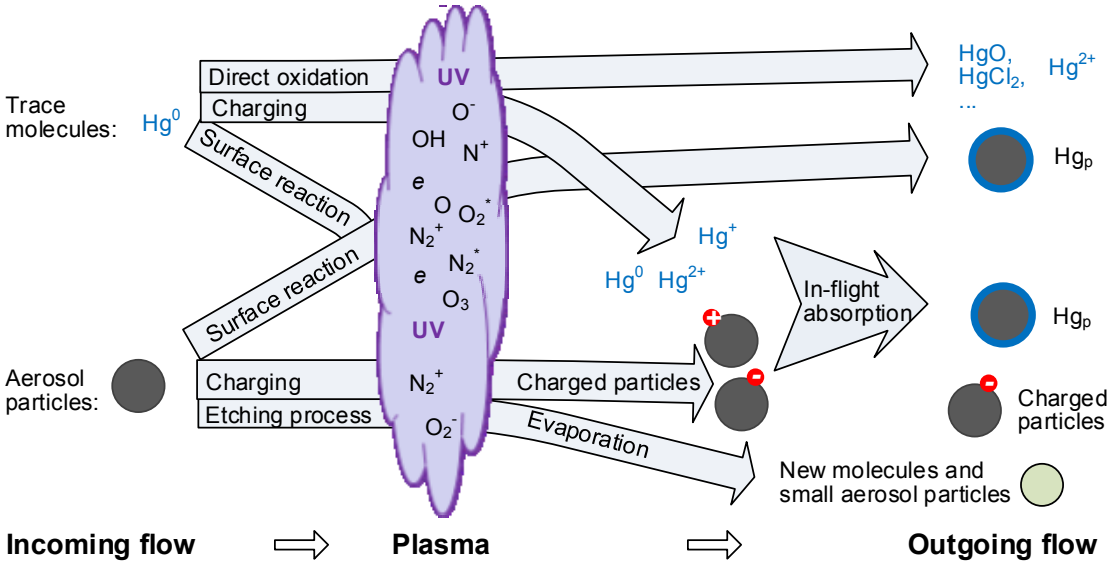

Fig. 6. Schematic illustration of Hg^0 removal mechanism with pre-existing aerosol particles in the plasma system. Three possible kinetic processes are responsible for Hg^0 removal, i.e., (i) directly oxidation by active species (such as •OH and O radicals) and etched out species (such as Cl from NaCl particle) to form oxidized mercury (Hg^{2+}); (ii) oxidation on particle surface to form particulate bound mercury (Hg_p); and (iii) in-flight adsorption by charged particles to form Hg_p.

possible that organic particles consume more reactive species than inorganic particles. This may explain different behaviors of inorganic particles (NaCl) and organic particles (sucrose) in improving Hg^0 removal efficiency. The practical kinetic processes can be more complex and remains to be further addressed.

SUMMARY

A double dielectric barrier discharge plasma device was developed for removing elemental mercury with the presence of aerosol particles. The existence of particles improves Hg^0 removal efficiency in plasma treatment process. Inorganic NaCl particles perform better than organic sucrose ones in improving Hg^0 removal efficiency. The plasma system also serves as an aerosol charger and an electrostatic precipitator such that these particles can be efficiently removed in the reactor. Three kinetic processes are possibly responsible for the improving Hg^0 removal efficiency: (i) rapid mercury oxidation by those etched out radical species from particle surfaces, (ii) mercury oxidation on the aerosol particle surface, and (iii) in-flight mercury adsorption by charged aerosol particles to form particulate bound mercury. These findings underline the important role of aerosol particles in mercury pollution controls. Further mechanism investigations are needed to reveal the role of suspended particles in the removal of mercury and other pollutants such as NO and volatile organic compounds.

ACKNOWLEDGEMENTS

We thank Qiang Zhang, Yang Qiao, Jiaxin Li, and Qingru Wu from Tsinghua University for their experimental supports. Q. Li thanks Profs. Reinhard Niessner, Dong Nam Shin, Herek L. Clack, Jie Li, and Da-Ren Chen for their helpful insights and discussions. Financial supports from the National Key Basic Research and Development Program of China (2013CB228505 & 2013CB43005), National High Technology Research and Development Program of China (2013AA065101 & 2013AA065004) and National Natural Science Foundation of China (21221004) are acknowledged.

REFERENCES

An, J.T., Shang, K.F., Lu, N., Jiang, Y.Z., Wang, T.C., Li, J. and Wu, Y. (2014). Performance Evaluation of Non-thermal Plasma Injection for Elemental Mercury Oxidation in a Simulated Flue Gas. *J. Hazard. Mater.* 268: 237–245.

Biswas, P., Senior, C., Chang, R., Vidic, R., Laudal, D. and Brown, T. (1999). Mercury Measurement and Its Control: What We Know, Have Learned, and Need to Further Investigate. *J. Air Waste Manage. Assoc.* 49: 1469–1473.

Byeon, J.H., Hwang, J.H., Park, J.H., Yoon, K.Y., Ko, B.J., Kang, S.H. J.J. (2006). Collection of Submicron Particles by an Electrostatic Precipitator Using a Dielectric Barrier Discharge. *J. Aerosol Sci.* 37: 1618–1628.

Byun, Y., Koh, D.J. and Shin, D.N. (2011a). Removal Mechanism of Elemental Mercury by Using Non-thermal Plasma. *Chemosphere* 83: 69–75.

Byun, Y., Koh, D.J., Shin, D.N., Cho, M. and Namkung, W. (2011b). Polarity Effect of Pulsed Corona Discharge for the Oxidation of Gaseous Elemental Mercury. *Chemosphere* 84: 1285–1289.

Chang, H.C. and Hsieh, L.T. (2013). Numerical Simulation of the Acenaphthylene Compound in an Atmospheric Plasma Reactor to Treat Cooking Fumes. *Aerosol Air Qual. Res.* 13: 122–136.

Chen, Z.Y., Mannava, D.P. and Mathur, V.K. (2006).

Mercury Oxidization in Dielectric Barrier Discharge Plasma System. *Ind. Eng. Chem. Res*. 45:6050–6055.

Clack, H.L. (2006). Mass Transfer within Electrostatic Precipitators: In-flight Adsorption of Mercury by Charged Suspended Particulates. *Environ. Sci. Technol.* 40: 3617–3622.

Clack, H.L. (2012). Estimates of Increased Black Carbon Emissions from Electrostatic Precipitators during Powdered Activated Carbon Injection for Mercury Emissions Control. *Environ. Sci. Technol.* 46: 7327–7333.

Granite, E.J. and Pennline, H.W. (2002). Photochemical Removal of Mercury from Flue Gas. *Ind. Eng. Chem. Res*. 41: 5470–5476.

Guo, S., Hu, M., Zamora, M.L., Peng, J.F., Shang, D.J., Zheng, J., Du, Z., Wu, Z., Shao, M., Zeng, L., Molina, M.J. and Zhang, R. (2014). Elucidating Severe Urban Haze Formation in China. *Proc. Nat. Acad. Sci. U.S.A.* 111: 17373–17378.

Jeong, J. and Jurng, J. (2007). Removal of Gaseous Elemental Mercury by Dielectric Barrier Discharge. *Chemosphere* 68:2007–2010.

Jia, B.J., Chen, Y., Feng, Q.Z. and Liu, L.Y. (2013). Research Progress of Plasma Technology in Treating NO, SO_2 and Hg^0 from Flue Gas. *Appl. Mech. Mater.* 295–298: 1293–1298.

Jiang, J., Hogan, C.J., Chen, D.R. and Biswas, P. (2007a). Aerosol Charging and Capture in the Nanoparticle Size Range (6-15 nm) by Direct Photoionization and Diffusion Mechanisms. *J. Appl. Phys*. 102: 034904.

Jiang, J., Lee, M.H. and Biswas, P. (2007b). Model for Nanoparticle Charging by Diffusion, Direct Photoionization, and Thermionization Mechanisms. *J. Electron. Test.* 65:209–220.

Jung, H. and Kittelson, D.B. (2005). Characterization of Aerosol Surface Instruments in Transition Regime. *Aerosol Sci. Technol.* 39:902–911.

Ko, K.B., Byun, Y., Cho, M., Namkung, W., Hamilton, I.P., Shin, D.N., Koh, D.J. and Kim, K.T. (2008). Pulsed Corona Discharge for Oxidation of Gaseous Elemental Mercury. *Appl. Phys. Lett.* 92: 251503.

Kuang, C., Riipinen, I., Sihto, S.L., Kulmala, M., McCormick, A.V. and McMurry, P.H. (2010). An Improved Criterion for New Particle Formation in Diverse Atmospheric Environments. *Atmos. Chem. Phys.* 10: 8469–8480.

Lee, T.G., Biswas, P. and Hedrick, E. (2004). Overall Kinetics of Heterogeneous Elemental Mercury Reactions on TiO_2 Sorbent Particles with UV Irradiation. *Ind. Eng. Chem. Res.* 43: 1411–1417.

Li, Q., Takana, H., Pu, Y.K. and Nishiyama, H. (2012). A Nonequilibrium Argon-oxygen Planar Plasma Jet Using a Half-confined Dielectric Barrier Duct in Ambient Air. *Appl. Phys. Lett.* 100:133501–133504.

Liang, X.H., Looy, P.C., Jayaram, S., Berezin, A.A., Mozes, M.S. and Chang, J.S. (2002). Mercury and Other Trace Elements Removal Characteristics of DC and Pulse-energized Electrostatic Precipitator. *IEEE Trans. Ind. Appl*. 38:69–76.

Lin, Y.C., Yang, P.M. and Chen, C.B. (2013). Reducing Emissions of Polycyclic Aromatic Hydrocarbons and Greenhouse Gases from Engines Using a Novel Plasma-enhanced Combustion System. *Aerosol Air Qual. Res.* 13: 1107–1115.

Liu, B.Y.H., Pui, D.Y.H., Rubow, K.L. and Szymanski, W.W. (1985). Electrostatic Effects in Aerosol Sampling and Filtration. *Ann. Occup. Hyg.* 29: 251–269.

Logager, T., Holcman, J., Sehested, K. and Pedersen, T. (1992). Oxidation of Ferrous-ions by Ozone in Acidic Solutions. *Inorg. Chem.* 31: 3523–3529.

Manirakiza, E., Seto, T., Osone, S., Fukumori, K. and Otani, Y. (2013). High-efficiency Unipolar Charger for Sub-10 nm Aerosol Particles Using Surface-discharge Microplasma with a Voltage of Sinc Function. *Aerosol Sci. Technol.* 47:60–68.

McLarnon, C.R., Granite, E.J. and Pennline, H.W. (2005). The Pco Process for Photochemical Removal of Mercury from Flue Gas. *Fuel Process. Technol.* 87:85–89.

McMurry, P.H., Fink, M., Sakurai, H., Stolzenburg, M.R., Mauldin, R.L., Smith, J., Eisele, F., Moore, K., Sjostedt, S., Tanner, D., Huey, L. G., Nowak, J. B., Edgerton, E., and Voisin, D. (2005). A Criterion for New Particle Formation in the Sulfur-rich Atlanta Atmosphere. *J. Geophys. Res.* 110: D22S02.

Pal, B. and Ariya, P.A. (2004). Studies of Ozone Initiated Reactions of Gaseous Mercury: Kinetics, Product Studies, and Atmospheric Implications. *Phys. Chem. Chem. Phys.* 6:572–579.

Romay, F.J., Liu, B.Y.H. and Pui, D.Y.H. (1994). A Sonic Jet Corona Ionizer for Electrostatic Discharge and Aerosol Neutralization. *Aerosol Sci. Technol.* 20: 31–41.

Saarnio, K., Frey, A., Niemi, J.V., Timonen, H., Rönkkö, T., Karjalainen, P., Vestenius, M., Teinilä, K., Pirjola, L., Niemelä, V., Keskinen, J., Häyrinen, A. and Hillamo, R. (2014). Chemical Composition and Size of Particles in Emissions of a Coal-fired Power Plant with Flue Gas Desulfurization. *J. Aerosol Sci.* 73: 14–26.

Sjostrom, S., Durham, M., Bustard, C.J. and Martin, C. (2010). Activated Carbon Injection for Mercury Control: Overview. *Fuel* 89: 1320–1322.

Suriyawong, A., Hogan, C.J., Jiang, J.K. and Biswas, P. (2008). Charged Fraction and Electrostatic Collection of Ultrafine and Submicrometer Particles Formed during O_2-CO_2 Coal Combustion. *Fuel* 87: 673–682.

Tsai, C.H., Tsai, P.S., Jou, C.J.G. and Liao, W.T. (2007). Conversion of Carbonyl Sulfide Using a Low-temperature Discharge Approach. *Aerosol Air Qual. Res.* 7: 251–259.

Wang, Z.H., Zhou, J.H., Zhu, Y.Q., Wen, Z.C., Liu, J.Z. and Cen, K. (2007). Simultaneous Removal of NO_x, SO_2 and Hg in Nitrogen Flow in a Narrow Reactor by Ozone Injection: Experimental Results. *Fuel Process. Technol.* 88: 817–823.

Wang, Z.H., Jiang, S.D., Zhu, Y.Q., Zhou, J.S., Zhou, J.H., Li, Z.S. and Cen, K.F. (2010). Investigation on Elemental Mercury Oxidation Mechanism by Non-thermal Plasma Treatment. *Fuel Process. Technol.* 91: 1395–1400.

Wu, C.Y., Lee, T.G., Tyree, G., Arar, E. and Biswas, P. (1998). Capture of mercury in Combustion Systems by in Situ-generated Titania Particles with UV Irradiation.

Environ. Eng. Sci. 15: 137–148.

Xu, F., Luo, Z.Y., Cao, W., Wang, P., Wei, B., Gao, X., Fang, M. and Cen, K. (2009). Simultaneous Oxidation of NO, SO_2 and Hg^0 from Flue Gas by Pulsed Corona Discharge. *J. Environ. Sci.-China* 21: 328–332.

Yang, H.M., Liu, H., Wu, H. and Wang, M. (2012). Photochemical Removal of Gaseous Elemental Mercury in a Dielectric Barrier Discharge Plasma Reactor. *Plasma Chem. Plasma Process.* 32:969–977.

Zhao, Y., Mann, M.D., Pavlish, J.H., Mibeck, B.A.F., Dunham, G.E. and Olson, E.S. (2006). Application of Gold Catalyst for Mercury Oxidation by Chlorine. *Environ. Sci. Technol.* 40: 1603–1608.

Received for review, January 4, 2015
Revised, March 12, 2015
Accepted, March 13, 2015